Biochemical and Biophysical Research Communications 446 (2014) 1190–1196

Contents lists available at ScienceDirect

Biochemical and Biophysical Research Communications

journal homepage: www.elsevier.com/locate/ybbrc

Transient increase in proteinuria, poly-ubiquitylated proteins and ER stress markers in podocyte-specific autophagy-deficient mice following unilateral nephrectomy

Juan Alejandro Oliva Trejo [a], Katsuhiko Asanuma [a,1], Eun-Hee Kim [a,2], Miyuki Takagi-Akiba [a], Kanae Nonaka [a], Teruo Hidaka [a], Masaaki Komatsu [b], Norihiro Tada [c], Takashi Ueno [d], Yasuhiko Tomino [a,*]

[a] Division of Nephrology, Department of Internal Medicine, Juntendo University School of Medicine, 2-1-1 Hongo, Bunkyo-ku, Tokyo 113-8421, Japan
[b] Protein Metabolism Project, Tokyo Metropolitan Institute of Medical Science, Setagaya-ku, Tokyo 156-8506, Japan
[c] Division of Genome Research, Research Institute for Diseases of Old Ages, Juntendo University School of Medicine, 2-1-1 Hongo, Bunkyo-ku, Tokyo 113-8421, Japan
[d] Laboratory of Proteomics and Biomolecular Science, Research Support Center, Juntendo University Graduate School of Medicine, 2-1-1 Hongo, Bunkyo-ku, Tokyo 113-8421, Japan

ARTICLE INFO

Article history:
Received 11 March 2014
Available online 26 March 2014

Keywords:
Autophagy
Atg7
Podocyte
Nephrectomy
Ubiquitin
ER stress

ABSTRACT

Previous studies have revealed that podocytes normally can be associated with a very high degree of autophagic activity, and that a lack of autophagic activity in podocytes is associated with susceptibility to disease and to late-onset glomerulosclerosis. In the present study, we conducted unilateral nephrectomy as a surgical model for acute nephron reduction. First, using GFP-LC3 transgenic mice to monitor autophagy, we found that glomerular autophagy could be transiently suppressed by surgery, but that it was restored quickly. To further explore the significance of podocyte autophagy after unilateral nephrectomy, we investigated podocyte-specific Atg7-deficient mice. The knockout mice exhibited no pathological phenotype compared with wild-type mice before nephrectomy. However, 1 day after nephrectomy, significantly higher levels of proteinuria and ultrastructural changes that included foot process effacement and a significant reduction in podocyte number were detected in mice harboring Atg7-deficient podocytes. Moreover, biochemical and immunohistochemical analyses showed a robust increase in polyubiquitin levels and ER stress markers in the glomeruli of the mice with autophagy-deficient podocytes. These results show the importance of the autophagic process in podocytes for maintaining a normal degree of filtration function during the adaptation to compensatory kidney hypertrophy following unilateral nephrectomy.

1. Introduction

Podocytes are highly specialized, visceral epithelial cells found in the glomerulus. They have unique primary processes emerging from the cell body, and many foot processes extend from each of the primary processes to wrap around capillaries [1,2]. The foot processes from two adjacent podocytes forms a slit membrane where blood is filtered and large molecules are held back. Thus, podocytes play an essential role in glomerular filtration. Animal models of drug-induced nephropathy and diabetic nephropathy have revealed a direct connection to podocyte injury and glomerulosclerosis that results in proteinuria [3,4].

Autophagy is a cellular degradative system involved in the turnover of cytoplasmic components via the lysosome. It significantly contributes to maintaining cell homeostasis by clearing denatured or injured cell constituents [5–7]. The impairment of autophagy has been associated with neurodegenerative disease and cancer [7], and autophagy has a protective role in kidney glomeruli [8]. In addition, podocytes exhibit high levels of basal autophagy [9,10], and podocyte autophagy plays a role in the recovery from glomerular injury induced by puromycin, lipopolysaccharides (LPS), and doxorubicin [9]. Recent studies using podocyte-specific autophagy-(Atg5)-deficient mice have revealed that a lack of

Abbreviations: UNX, unilateral nephrectomy/uninephrectomy; GFP, green fluorescent protein; mTor, mammalian target of rapamycin.

* Corresponding author. Fax: +81 3 3813 1183.
E-mail address: yasu@juntendo.ac.jp (Y. Tomino).
[1] Present address: Laboratory for Kidney Research (TMK Project), Medical Innovation Center, Kyoto University Graduate School of Medicine, 53 Shogoin Kawaharacho, Sakyo-ku, Kyoto 606-8397, Japan.
[2] Present address: Osong Medical Innovation Foundation, Laboratory Animal Center, Osong Saengmyung-ro 123, Osong-eub, Cheongwon-gun, Chungbuk 363-951, Republic of Korea.

http://dx.doi.org/10.1016/j.bbrc.2014.03.088
0006-291X/

autophagy results in higher sensitivity to the aforementioned substances, causing late-onset glomerulosclerosis [11].

Unilateral nephrectomy (UNX) is a surgical procedure to remove a contralateral kidney. Immediately following UNX, both functional and structural loads act on the remaining kidney under a state of hyperfiltration [12,13]. Depending on many different factors, including age [14,15] and genetic manipulation [16], UNX could frequently lead to glomerulosclerosis and proteinuria. In view of the importance of podocyte autophagy in glomerular filtration, it is important to investigate whether UNX has an effect on glomeruli that harbor autophagy-deficient podocytes. Here we report anatomical, physiological, and molecular changes in the adaptation processes of the remaining glomeruli when we used the UNX model on podocyte-specific Atg7-deficient mice.

2. Materials and methods

2.1. Antibodies

We used the following commercially available antibodies: monoclonal guinea pig anti-p62 and polyclonal guinea pig anti-Nephrin from PROGEN (Heidelberg, Germany); polyclonal rabbit anti-ubiquitin from DAKO (California, USA); monoclonal mouse anti-PA28α from MBL (Nagoya, Japan); mouse monoclonal anti-proteasome 20S subunit alpha and beta from Enzo Life Sciences (New York, USA); rabbit monoclonal anti-ribosomal S6, phosphorylated-S6 antibodies, rabbit polyclonal anti-calnexin, Bip, p53, eIF2-alpha, phosphorylated-eIF2-alpha antibodies, and mouse monoclonal anti-GAPDH antibody from Cell Signaling Technology (Massachusetts, USA). Anti-Atg7 and anti-LC3 antibodies were prepared as previously described [17].

2.2. Mouse models

Podocyte-specific Atg7-deficient mice were generated by crossing previously described *Atg7*$^{flox/flox}$ mice [17] with podocin-Cre mice [18]. The littermates lacking podocin-Cre were used as control wild-type mice. GFP-LC3 mice have been previously described [10]. All mice were housed and bred in environmentally controlled rooms, with free access to water and a normal pelleted diet. All animal experiments were guided and approved by the Committee for Animal Experiments of Juntendo University.

2.3. Primary podocytes

Primary podocytes were isolated from glomeruli that had been separated from kidneys using a graded sieving method, as previously described [19]. The podocytes were maintained with RPMI/10% FCS.

2.4. Unilateral nephrectomy

Unilateral nephrectomy was performed, as previously described [20].

2.5. Proteinuria measurement

Mouse urine was collected daily and analyzed using DCA 2000 microalbumin-creatinine immunoassay cartridges with a DCA Vantage Analyzer (Siemmens Healthcare, Erlangen, Germany). Proteinuria was expressed as the albumin (mg) to creatinine (g) ratio [21].

2.6. Renal histology and immunohistochemistry

Kidneys were fixed via the ventricular perfusion of 4% paraformaldehyde and embedded in paraffin. Kidney sections (3 μm thick) were stained with a periodic acid–Schiff (PAS) reagent or with primary antibodies followed by the respective secondary antibodies. All histological and immunohistochemical specimens were observed using a light microscope (Olympus BX41; Olympus, Japan). To determine the glomerulus to Bowman's capsule ratio, PAS-stained Bowman's capsules (more than 30 capsules per mouse and 4 mice per each experimental group) were analyzed using a KS-400 Imaging System, as previously described [21].

2.7. Foot process effacement

Foot process effacement is assessed as the rate of effacement, which is determined as the length of the effacement divided by the length of the capillary, as previously described [22]. We measured 4–5 glomeruli per mouse and 4–5 capillaries per glomerulus for 3 mice in each experimental group.

2.8. Immunofluorescence staining

Kidneys from GFP-LC3 transgenic mice were processed as previously described [23]. Kidney sections (3 μm thick) stained with DAPI were counterstained with anti-Lamp1 antibody. More than 15 random glomerulus pictures per mouse for a total of 3 mice from each experimental group were taken without changing the exposure settings. The GFP-LC3 dots and immunofluorescence of Lamp1 were analyzed using a confocal fluorescence microscope (Olympus FV1000; Olympus, Japan). The data were quantified using Image J software.

2.9. Counting the podocytes per glomerulus

Kidney sections (3 μm thick) were double-stained with DAPI and anti-WT antibody. More than 60 glomeruli per experimental group (4 mice per group) were analyzed for counting double-positive cells (podocytes) using a confocal microscope (Olympus FV1000; Olympus, Japan).

2.10. Western blotting (WB)

Glomeruli were isolated from kidneys using a graded sieving method. Isolated glomeruli and cultured podocytes were processed for Western blotting, as previously reported [19,24].

2.11. Statistical analysis

Statistical significance between the two groups was evaluated using a Student's *t* test and determined as statistically significant when $p < 0.05$. Values were expressed as the mean ± SEM.

3. Results

3.1. Autophagy was downregulated temporarily on day 1 after UNX but was restored quickly in glomeruli

To assess autophagy in kidney glomeruli during recovery from UNX, we first performed UNX on GFP-LC3 transgenic mice expressing the fluorescent autophagosomal membrane marker GFP-LC3. Before UNX, numerous fluorescent dots corresponding to autophagosomes could be seen in the glomeruli (Fig. 1A). Most of the dots delineated a podocyte pattern, and therefore seemed attributable to podocytes (high magnification) [9,19]. Immediately after UNX, the numbers of glomerular GFP-LC3 dots had reduced significantly (Fig. 1A day 1), but then the numbers recovered almost to the initial levels before surgery on day 3 (Fig. 1A and B), which suggested a temporary decrease in autophagosomes after UNX.

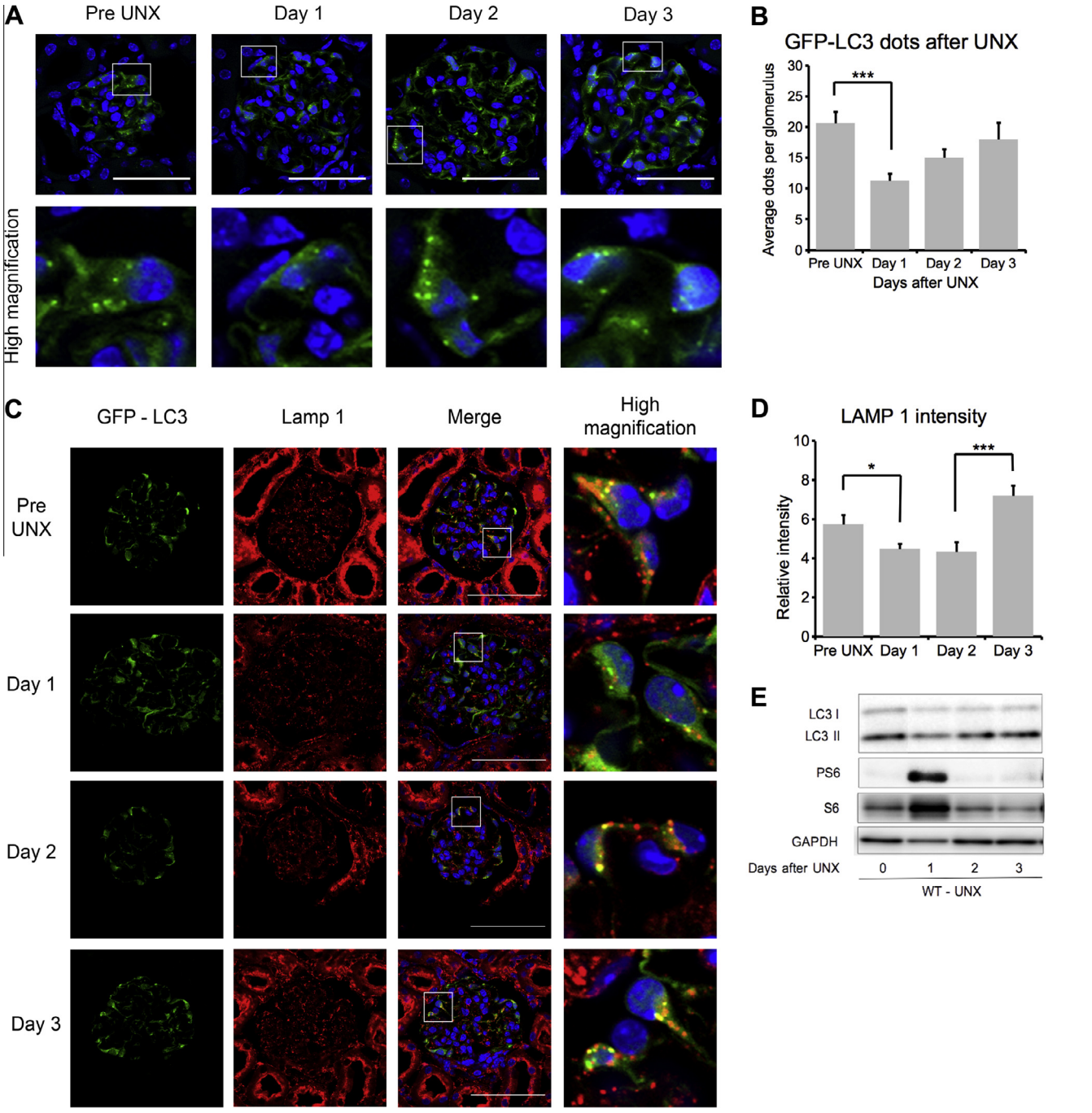

Fig. 1. Autophagy is downregulated temporarily on day 1 following UNX but is restored quickly afterwards for podocytes. (A) Fluorescent micrographs of glomeruli from GFP-LC3 mice stained with Hoechst33342 (nuclei, blue) before and after UNX. Boxed areas including podocytes at higher magnification are presented in the lower panels. (bar, 50 μm). (B) Number of GFP LC3 dots per glomeruli of GFP-LC3 mice. More than 15 glomeruli per mouse and 3 mice per day were examined (means ± S.D., $^{***}p < 0.001$, day 1 vs. pre UNX). (C) Fluorescent micrographs of glomeruli of GFP-LC3 mice immunostained with anti-Lamp1 antibody (red). Boxed areas including podocytes at higher magnification are presented on the right (bar, 50 μm). (D) Lamp1 intensity per glomeruli on GFP-LC3 mice before and after UNX. More than 4 glomeruli per mouse and 3 mice per day were examined (means ± S.D., $^{*}p < 0.05$, day 1 vs. pre UNX; $^{\#\#\#}p < 0.001$, day 2 vs. day 3). (E) Western blotting analysis of LC3, p62, S6, phosphorylated S6 (PS6) in glomerular lysates prepared from wild type mice before and after UNX.

Concomitantly, Lamp1, a lysosomal marker, decreased in the glomeruli during days 1–2 following UNX, but then there was a significant increase on day 3 (Fig. 1C and D). In the merged figures under high magnification, a decrease in the colocalization of LC3 dots with Lamp1 dots in podocytes was seen on day 1, indicating a suppression of autophagosomal lysosomal turnover (autophagy flux).

UNX stimulated a compensatory hypertrophy of the remaining portions of the kidneys, including both renal tubules and the glomeruli [12,13], and this hypertrophy activated other forms of cell proliferative signaling, such as mammalian targets of rapamycin (mTor) [20]. WB analysis of glomerular lysates showed that ribosomal S6, a downstream effecter of mTor, was strongly phosphorylated on day 1 (Fig. 1E). Thus, our observations of autophagy suppression in podocytes immediately after UNX were consistent with mTor activation under compensatory hypertrophic conditions.

3.2. UNX produces functional and ultrastructural changes in Atg7-deficient podocytes and glomeruli that result in mild podocyte loss

Because autophagy in podocytes appeared to be downregulated on day 1 after UNX, we hypothesized that podocyte autophagy was dispensable during the initial stage of compensatory glomerular hypertrophy after UNX. To test this hypothesis, we performed UNX on podocyte-specific autophagy (Atg7)-deficient mice. We generated podocyte-specific Atg7 mice as described in Section 2. In Fig. 2A, Atg7 was immunoprecipitated from glomerular lysates of wild type, heterozygous, and knockout mice, and the precipitates were probed with anti-Atg7 antibody using WB analysis (Fig. 2A). A significant reduction in Atg7 (~40%) was confirmed in the glomeruli of podocyte-specific Atg7-deficient mice compared with those of wild type and heterozygous mice. Since podocyte protein accounts for ~30–40% of total glomerular protein, the data were consistent with Atg7-deficiency in podocytes. We next isolated primary podocytes from knockout mice and wild type littermates and used WB to analyze the Atg7. As shown in Fig. 2A, a complete lack of Atg7 in primary podocytes from knockout mice, was confirmed.

Prior to UNX, podocyte-specific Atg7-deficient mice looked virtually identical to wild type mice when comparing weight and proteinuria at 3 months of age (Fig. 2B). We then performed UNX and monitored the proteinuria levels for 3 days after surgery on both groups. Contrary to our assumptions, we found increased damage to the podocytes of Atg7-deficient mice, as evidenced by higher proteinuria levels on day 1 following UNX (Fig. 2C). However, the levels of proteinuria for Atg7-deficient mice had returned to almost normal levels by day 3 and no significant difference could be detected between the two groups (Fig. 2C). As higher proteinuria is most likely attributable to podocyte damage in the absence of Atg7, we next compared the ultrastructures of the glomeruli from both groups using an electron microscope (Fig. 2D). On day 1 following UNX, podocytes with overstretched bodies and pseudocysts were frequently observed. There was an apparent increase in foot process effacement in Atg7-deficient mice (Fig. 2D, arrows). Again, however, by day 3 following UNX, no detectable differences existed between the two groups. To corroborate our day 1 observations, we measured the rate of effacement and found significantly more foot process effacement of Atg7-deficient podocytes (Fig. 2E). We then analyzed PAS-stained kidney samples from both groups to compare the morphological changes (Fig. 2F). We found no obvious pathological symptoms in the glomeruli harboring Atg7-deficient podocytes before UNX. However, the glomerulus to Bowman space ratio of Atg7-deficient mice was larger than that of wild type mice on day 1 (Fig. 2F and G). These results show that glomeruli harboring Atg7-deficient podocytes expanded more widely compared with wild type glomeruli immediately after UNX, suggesting that an Atg7-deficiency of podocytes causes vulnerability in glomeruli that are under the increased pressure of hyperfiltration.

To evaluate whether these changes had an impact on podocyte viability, we counted the podocytes from both groups (Fig. 2H). There was no difference either prior to UNX (Fig. 2H) or on day 1 (data not shown) following UNX. However, by day 3, the podocyte number had decreased significantly for Atg7-deficient mice, suggesting that Atg7-deficient podocytes have greater difficulty enduring a glomerular filtration load during the compensatory growth of the remaining glomeruli following UNX.

3.3. UNX elicits an accumulation of polyubiquitin and an increase in the ER stress response in the glomeruli of Atg7-deficient mice

As established previously [8,25], a higher level of p62 was present in the glomeruli of podocyte-specific Atg7-deficient mice compared with levels in wild type mice (Fig. 3A), and the aforementioned levels were further increased on day 1 following UNX. It is noteworthy that a dramatic increase in polyubiquitylated proteins in the glomeruli of Atg7-deficient podocytes was seen on day1 following UNX (Fig. 3A). It was also noted that 26S proteasome subunits, including α, β, and PA28α, increased coincidentally with polyubiquitin on day 1 (Fig. 3A). The accumulation of polyubiquitylated proteins is a hallmark of proteasome impairment. In fact, p53, a substrate for proteasome, increased significantly on day 1 in the glomeruli harboring Atg7-deficient podocytes (Fig. 3B). Immunohistochemistry revealed that podocytes were strongly positive with polyubiquitin staining compared with other parts in the glomeruli on day 1 (Fig. 3B). These results suggest that proteasome function was transiently impaired in Atg7-deficient podocytes immediately following UNX (day 1), but was recovered afterwards. The increased levels of 26S proteasome subunits on day1 were most likely due to a counteractive response to mitigate the accumulation of polyubiquitin in podocytes.

During the compensatory hypertrophy following UNX, protein synthesis was upregulated in the remaining renal tubules as well as in glomeruli [26]. As shown in Fig. 3A, BiP and phosphorylated eIF2α was markedly increased in glomeruli of Atg7-deficient podocytes but not in wild type glomeruli following UNX, indicating significant ER stress was elicited in the glomeruli harboring Atg7-deficient podocytes. Thus, an autophagy deficiency in podocytes causes ER stress during compensatory hypertrophy with decreased proteasomal degradation, which results in the accumulation of polyubiquitylated proteins.

4. Discussion

UNX stimulates compensatory hypertrophy in the remaining kidney, for which the workload is increased for the remaining tubular and glomerular cells in order to maintain normal kidney functions (hyperfiltration). Most of the growth in the remaining kidney can be attributed to tubular cells [13], but the glomeruli also undergo growth, because the inability for glomeruli to grow is detrimental to the kidney [14,15]. The cell growth begins as early as several hours following UNX [26]. The expected response is an increase in protein synthesis to increase cell volume. Indeed, our data from the WB of glomerular lysate (Fig. 3) clearly support the previous data showing that mTor activation plays a role in kidney growth following UNX [20]. Conversely, using GFP-LC3 transgenic mice, we confirmed that autophagy was significantly suppressed immediately following UNX (day 1) under the conditions of mTor activation (Fig. 1). Thus, autophagy apparently did not appear to play a role in the podocytes immediately following UNX, so it was assumed that the glomeruli harboring autophagy-deficient podocytes would show no pathological phenotypes following UNX. To our surprise, however, podocyte-specific Atg7-deficient mice exhibited a significantly higher level of proteinuria than the wild type control mice on day 1 following UNX. This phenotype could have been attributable to a dysfunction of the glomeruli harboring Atg7-deficient podocytes, because significantly larger structural changes of the glomeruli, such as foot process effacements and larger glomerulus to Bowman space ratios, were elicited on day 1 following UNX. Hence, even at the lowest levels on day 1, podocyte autophagy is necessary for glomeruli to maintain a proper adaptation to the initial step of the compensatory process following UNX. In other words, a lack of podocyte autophagy significantly retards this process.

In the present study, WB analyses of glomerular lysate revealed a dramatic accumulation of poly-ubiquitylated proteins, and increased levels of p62, proteasome subunits, and ER stress markers

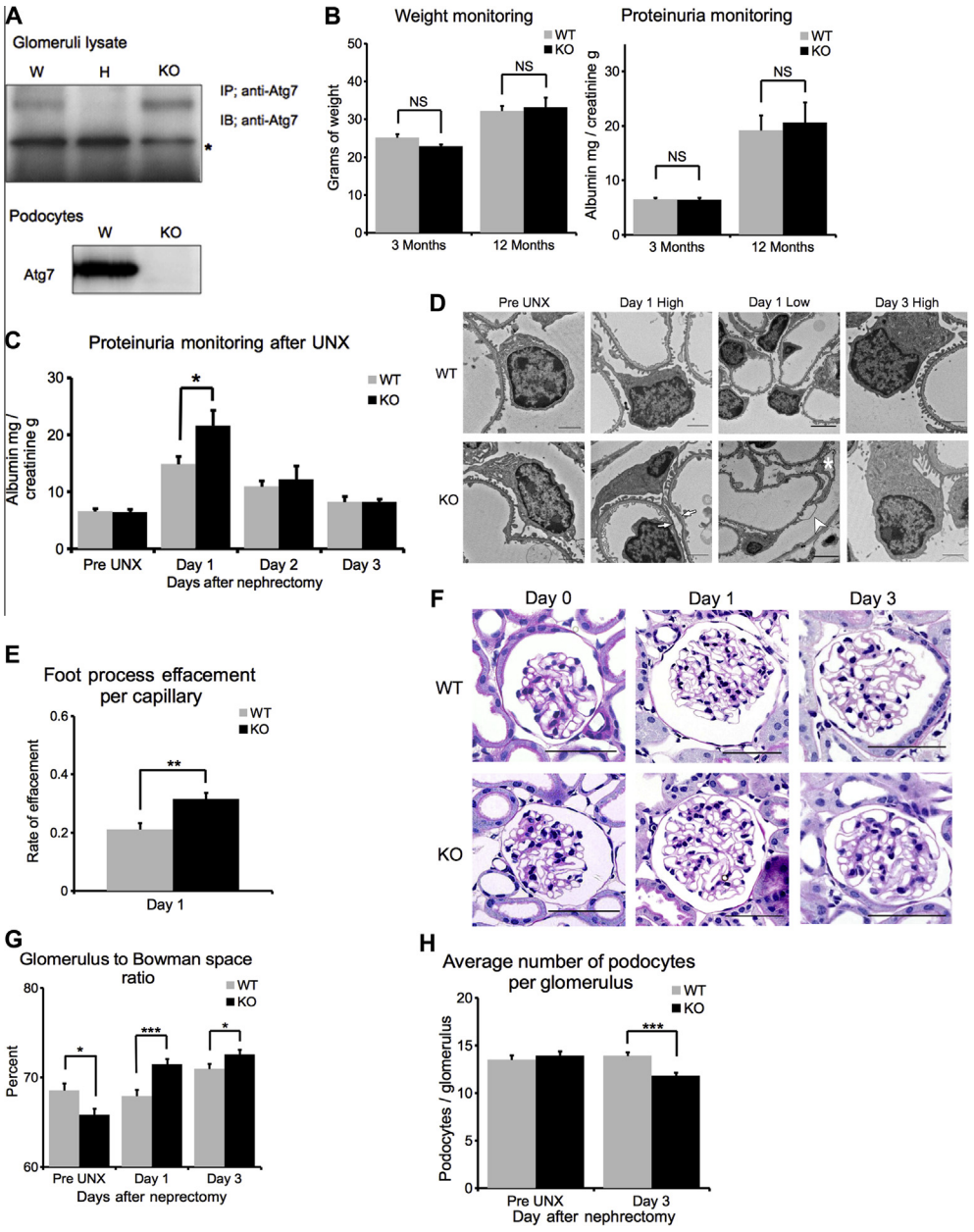

Fig. 2. UNX causes pathological and ultrastructural changes of the glomeruli as well as podocyte loss in podocyte-specific Atg7-deficient mice. (A) Upper panel: Atg7 was immunoprecipitated from the glomerular lysate (300 μg protein) of wild type, heterozygous, and podocyte-specific Atg7-deficient mice, respectively. The precipitates were separated on 7.5% SDS–PAGE gels and separated polypeptides were subjected to WB analysis for detecting Atg7 (*). Lower panel: Primary podocytes were isolated from the glomeruli fractions of wild type and podocyte-specific Atg7-deficient mice, respectively, and subjected to WB analysis for Atg7. (B) Body weight (gram) of wild type and podocyte-specific Atg7-deficient mice at 3 and 12 months of age (left) (means ± S.D., $n \geqslant 4$, NS, not significant). Albuminuria levels in wild type and podocyte-specific Atg7-deficient mice at 3 and 12 months of age (right) (means ± S.D., NS, not significant). (C) Changes in proteinuria levels in wild type and podocyte-specific Atg7-deficient mice prior to UNX and days 1, 2, and 3 following UNX ($n \geqslant 8$ mice per group; means ± S.D., $^{*}p < 0.05$, knockout mice vs. wild type mice on day 1). (D) Electron micrographs of the glomeruli of wild type mice and those harboring Atg7-deficient podocytes prior to UNX, days 1, and day 3 following UNX. Arrows indicate the areas of foot process effacement, the star indicates pseudocyst and the arrowhead indicates an overstretched podocyte body. (bar, 2 μm). (E) Quantification of foot process effacement per capillary. ($n = 3$ per group, 4–5 glomeruli and capillaries per mouse; $^{**}p < 0.01$, wild type vs. knockout mice). (F) PAS stained glomeruli of wild type and podocyte-specific Atg7-deficient mice prior to and following UNX. (bar, 50 μm). (G) Glomerulus-to-Bowman-space ratio measured prior to and following UNX. ($n \geqslant 30$ glomeruli per mouse and 4 mice per group; means ± S.D. $^{*}p < 0.05$, knockout mice vs. wild type mice prior to UNX and by day 3 following surgery; $^{***}p < 0.001$, knockout mice vs. wild type mice on day 1). (H) Average number of podocytes per glomerulus prior to UNX and 3 days following surgery. More than 15 glomeruli per mouse and 4 mice per group were investigated; $^{***}p < 0.001$, knockout vs. wild type mice.

on day 1 following UNX in Atg7-deficient mice (Fig. 3A). Immunohistochemistry indicated that polyubiquitylated proteins most likely accumulated in the podocytes (Fig. 3B), strongly suggesting proteasome dysfunction had occurred in the podocytes. Consistently, p53, a proteasome substrate, was increased on day 1 following UNX. Prior to UNX and on days 2–3 following UNX, no obvious accumulation of polyubiquitylated proteins had occurred in the glomeruli of either control or Atg7-deficient mice. Therefore, the accumulation of polyubiquitylated proteins appeared to be triggered by UNX, which somehow induced a transient inhibition of proteasome under autophagy deficiency. It was noteworthy that a marked elevation in ER stress was shown by increases in BiP and in phosphorylated eIF-2α. In compensatory hypertrophy, protein synthesis to grow the remaining kidney is robustly enhanced. Under these conditions,

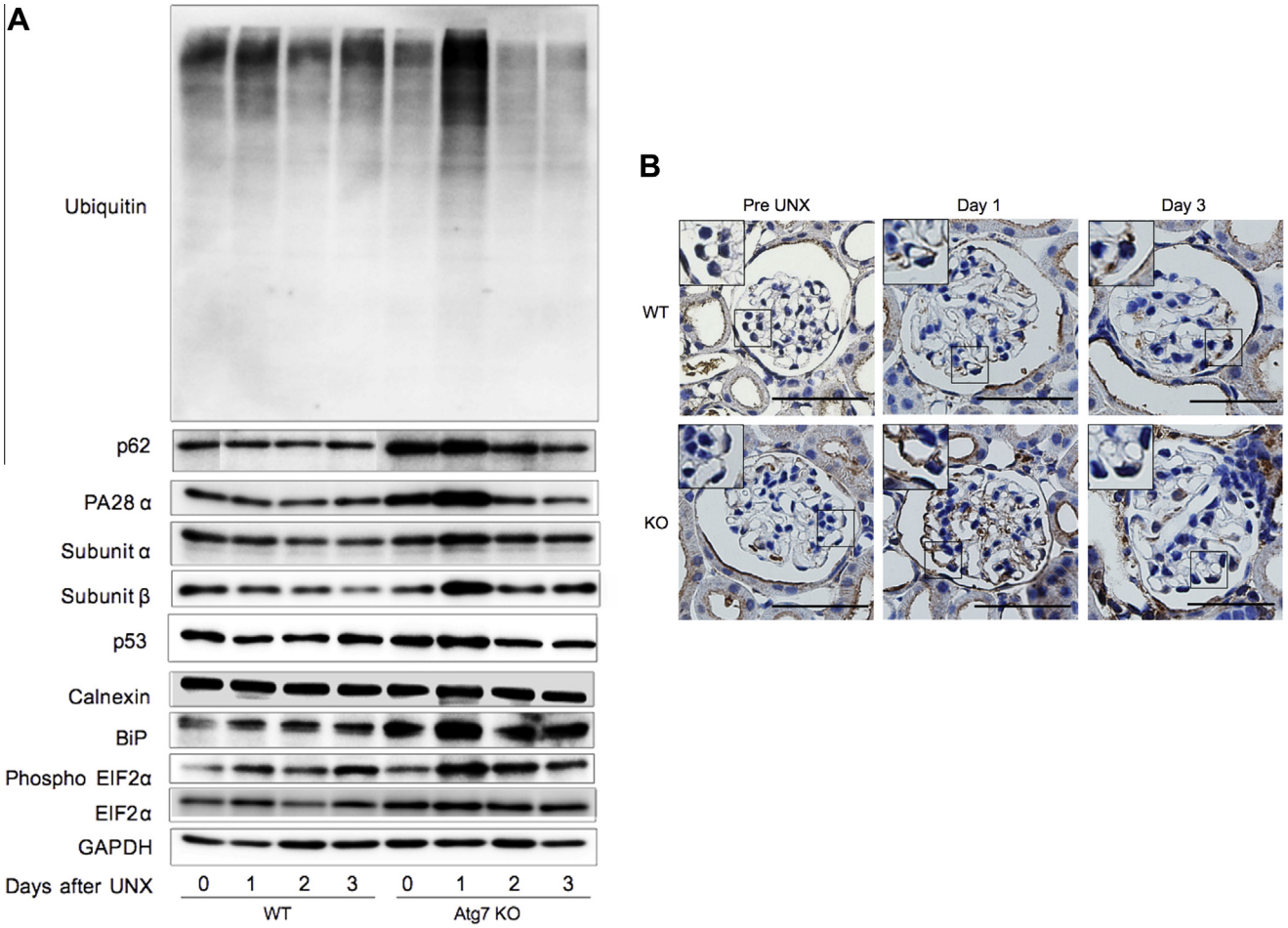

Fig. 3. Accumulation of poly-ubiquitylated polypeptides in podocytes and increase in ER stress markers in the glomeruli of podocyte-specific Atg7-deficient mice following UNX. (A) Western blotting analysis of polyubiquitin, regulatory subunit of 26S proteasome (PA28α), 20 s proteasome subunits α and β, p53, and ER stress markers (calnexin, BiP, eIF-2α, phosphorylated eIF-2α), in glomerular lysates isolated from wild type and podocyte-specific Atg7-deficient mice. (B) Immunohistochemical distribution of ubiquitin in the glomerulus from wild type and podocyte-specific Atg7-deficient mice prior to and days 1 and 3 following UNX. Insert shows areas including podocytes under higher magnification (bar, 50 μm).

quality control of newly synthesized proteins in the ER lumen must be accomplished by ER-associated-degradation (ERAD) and ER-activated autophagy [27]. The enhanced ER stress response in Atg7-deficient podocytes may reflect a defective ERAD under both autophagy deficiency and compensatory hypertrophic conditions. In this respect, our data are consistent with results reported by Korolchuk et al. [28], which showed that the degradation of proteasome substrates is compromised under autophagy inhibition.

In the present study, these pathological symptoms did not continue, and glomerular function of the remaining kidney was restored to its normal state within a couple of days. That result shows that basal podocyte autophagy is necessary for promoting the initial process of hypertrophy following UNX, but not for the later stages of compensatory hypertrophy. We measured proteinuria and glomerular morphometry for 150 days following UNX. Apparently, there was no significant difference between wild type and podocyte-specific Atg7-deficient mice. However, an injection of lipopolysaccharide to mice 150 days following UNX induced a greater degree of proteinuria in the knockout mice than in the wild type mice (Oliva Trejo JA, Takagi-Akiba M, Asanuma K, Ueno T, Tomino, Y, unpublished observation). This indicated that autophagy-deficient podocytes retain a potential vulnerability to those external stimuli that are known to target podocytes and cause glomerular nephropathy, as reported by Hartleben et al. [8].

Conflicts of interest

The authors declare that they have no conflicts of interest.

Acknowledgments

We thank Dr. Lu Hongmei for teaching us the unilateral nephrectomy technique; Laboratory of Molecular and Biochemical Research, Research Support Center, Ms. Terumi Shibata, Ms. Kaori Takahashi, Mr. Junichi Nakamoto, and Mr. Mitsutaka Yoshida all from the Juntendo University Graduate School of Medicine, Tokyo, Japan, for their excellent technical assistance. This work was supported in part by a Grant-in-Aid for Young Scientists (19890213 to KA, 24790856 to MT-A) , Grants-in-Aid for Scientific Research (C, 23591201 to KA) , a Grant-in-Aid for Challenging Exploratory Research (21659217 to KA) , a Grant-in-Aid for Scientific Research on Priority Areas (18076005 to TU, MK) , a Grant-in-Aid for the "High-Tech 425 Research Center" Project for Private Universities, a matching fund subsidy (O-TJ, TU, YT) from the Ministry of Education, Culture, Sports, Science and Technology (MEXT) of Japan, a Grant-in-Aid for the Third-Term Comprehensive 10-Year Strategy for Cancer Control from the Ministry of Health, Labor, and Welfare (16271401 to TU). This work was also supported by Research Grants from the Takeda Science Foundation (KA, TU), the Kanae

Foundation for the Promotion of Medical Science (KA), and the Kowa Life Science Foundation (KA). The authors thank Dr. James McDonald for language editing.

References

[1] P. Mundel, W. Kriz, Structure and function of podocytes: an update, Anat. Embryol. (Berl) 192 (1995) 385–397.
[2] H. Pavenstädt, W. Kriz, M. Kretzler, Cell biology of the glomerular podocyte, Physiol. Rev. 83 (2003) 253–307.
[3] K. Asanuma, P. Mundel, The role of podocytes in glomerular pathobiology, Clin. Exp. Nephrol. 7 (2003) 255–259.
[4] F.N. Ziyadeh, G. Wolf, Pathogenesis of the podocytopathy and proteinuria in diabetic glomerulopathy, Curr. Diabetes Rev. 4 (2008) 39–45.
[5] N. Mizushima, M. Komatsu, Autophagy: renovation of cells and tissues, Cell 147 (2011) 728–741.
[6] P. Boya, F. Reggiori, P. Codogno, Emerging regulation and functions of autophagy, Nat. Cell Biol. 15 (2013) 713–720.
[7] N. Mizushima, B. Levine, A.M. Cuervo, D.J. Klionsky, Autophagy fights disease through cellular self-digestion, Nature 451 (2008) 1069–1075.
[8] B. Hartleben, N. Wanner, T.B. Huber, Autophagy in glomerular health and disease, Semin. Nephrol. 34 (2014) 42–52.
[9] K. Asanuma, I. Tanida, I. Shirato, et al., MAP-LC3, a promising autophagosomal marker, is processed during the differentiation and recovery of podocytes from PAN nephrosis, FASEB J. 17 (2003) 1165–1167.
[10] N. Mizushima, A. Yamamoto, M. Matsui, et al., In vivo analysis of autophagy in response to nutrient starvation using transgenic mice expressing a fluorescent autophagosome marker, Mol. Biol. Cell 15 (2004) 1101–1111.
[11] B. Hartleben, M. Gödel, C. Meyer-Schwesinger, et al., Autophagy influences glomerular disease susceptibility and maintains podocyte homeostasis in aging mice, J. Clin. Invest. 120 (2010) 1084–1096.
[12] L.G. Wesson, Compensatory growth and other growth responses of the kidney, Nephron 51 (1989) 149–184.
[13] L.G. Fine, J.T. Norman, Renal growth responses to acute and chronic injury: routes to therapeutic intervention, J. Am. Soc. Nephrol. 2 (1992) S206–S211.
[14] M. Nagata, K. Schärer, W. Kriz, Glomerular damage after uninephrectomy in young rats. I. Hypertrophy and distortion of capillary architecture, Kidney Int. 42 (1992) 136–147.
[15] M. Nagata, W. Kriz, Glomerular damage after uninephrectomy in young rats. II. Mechanical stress on podocytes as a pathway to sclerosis, Kidney Int. 42 (1992) 148–160.
[16] A. Fukuda, M.A. Chowdhury, M.P. Venkatareddy, et al., Growth-dependent podocyte failure causes glomerulosclerosis, J. Am. Soc. Nephrol. 23 (2012) 1351–1363.
[17] M. Komatsu, S. Waguri, T. Ueno, et al., Impairment of starvation-induced and constitutive autophagy in Atg7-deficient mice, J. Cell Biol. 169 (2005) 425–434.
[18] M.J. Moeller, S.K. Sanden, A. Soofi, et al., Podocyte-specific expression of cre recombinase in transgenic mice, Genesis 35 (2003) 39–42.
[19] M. Takagi-Akiba, K. Asanuma, I. Tanida, et al., Doxorubicin-induced glomerulosclerosis with proteinuria in GFP-GABARAP transgenic mice, Am J. Physiol. Renal Physiol. 302 (2012) F380–F389.
[20] J.K. Chen, J. Chen, E.G. Neilson, et al., Role of mammalian target of rapamycin signaling in compensatory renal hypertrophy, J. Am. Soc. Nephrol. 16 (2005) 1384–1391.
[21] M. Tanimoto, Q. Fan, T. Gohda, et al., Effect of pioglitazone on the early stage of type 2 diabetic nephropathy in KK/Ta mice, Metabolism 53 (2004) 1473–1479.
[22] J.K.J. Deegens, H.B.P.M. Dijkman, G.F. Borm, et al., Podocyte foot process effacement as a diagnostic tool in focal segmental glomerulosclerosis, Kidney Int. 74 (2008) 1568–1576.
[23] N. Mizushima, Methods for monitoring autophagy using GFP-LC3 transgenic mice, Methods Enzymol. 452 (2009) 13–23.
[24] K. Asanuma, E. Yanagida-Asanuma, C. Faul, et al., Synaptopodin orchestrates actin organization and cell motility via regulation of RhoA signalling, Nat. Cell Biol. 8 (2006) 485–491.
[25] M. Komatsu, S. Waguri, M. Koike, et al., Homeostatic levels of p62 control cytoplasmic inclusion body formation in autophagy-deficient mice, Cell 131 (2007) 1149–1163.
[26] I. Sinuani, I. Beberashvili, Z. Averbukuh, et al., Mesangial cells initiate compensatory tubular cell hypertrophy, Nephrology 31 (2010) 326–331.
[27] H. Digaleh, M. Kiaei, F. Khodagholi, Nrf2 and Nrf1 signaling and ER stress crosstalk: implication for proteasomal degradation and autophagy, Cell. Mol. Life Sci. 70 (2013) 4681–4694.
[28] V.I. Korolchuk, A. Mansilla, F.M. Menzies, et al., Autophagy inhibition compromises degradation of ubiquitin–proteasome pathway substrates, Mol. Cell. 33 (2009) 517–527.